Charge-Transfer Formation and Geometry of the Naphthalene−Trimethylamine van der Waals Complex

Darren P. Andrews,‡ Godfrey S. Beddard,* and Benjamin J. Whitaker

School of Chemistry, University of Leeds, Leeds LS2 9JT, U.K.

Received: March 17, 2000; In Final Form: May 15, 2000

Spectroscopic and kinetic experiments on the naphthalene−trimethylamine van der Waals (vdW) complex in a molecular beam are described. When the complex is vibronically excited, as well as a small amount of fluorescence characteristic of naphthalene, a broad, featureless, red-shifted emission is observed. This is attributed to fluorescence from an excited charge-transfer (CT) state of the cluster. Unlike naphthalene−triethylamine, the trimethylamine complex has absorption transitions with measurable rotational structure, and approximate rotational constants of 490, 500, and 900 ± 50 MHz were obtained. The rise time of the CT emission is ∼60 ps when excited into the $S_1 + 455$ cm^{-1}, $8(b_{1g})^1$, naphthalene transition, and its decay lifetime is 56 ± 3 ns. This lifetime increases as the excitation energy increases to reach 105 ± 5 ns at $S_1 + 1131$ cm^{-1}, $8(b_{1g})^1 8(a_g)^1$, which is the opposite trend to that which is observed in other naphthalene−amine complexes. The geometry of the complex was determined from the rotational constants and by ab initio calculations. The amine was found to lie symmetrically disposed about the naphthalene long axis and above one of the naphthalene rings, with its hydrogen atoms toward the naphthalene. The results are interpreted in terms of the crossing of the initial locally excited (LE) state of the vdW complex, which has mainly naphthalene character, to the CT state.

Introduction

Excitation of the locally excited (LE) state of an electron donor, D, and acceptor, A, van der Waals (vdW) complex can lead to an excited charge-transfer (CT) state D^+A^-, also called an exciplex. In the condensed phase it has been known for about 30 years that naphthalene, like many other aromatics, forms exciplexes with numerous amines, both inter- and intramolecularly, but not until 1982 was the first observation of fluorescence from a CT state in a free jet reported by Russell and Levy.[1] The extent of exciplex formation was observed by monitoring fluorescence-excitation spectra, and single-vibronic-state lifetimes were obtained. This observation was shortly followed by others,[2] and in 1-cyanonaphthalene−triethylamine, exciplex formation was shown to be generally more favorable at higher vibrational energies.[3,4]

Saigusa et al.[5] made the interesting observation that an $S_1 + 402$ cm^{-1} mode produced naphthalene-like emission, but the $S_1 + 402 + 10$ cm^{-1} combination mode, formed with a ∼10-cm^{-1} intermolecular vibration, showed exciplex emission, thus identifying the promoting mode for the reaction, $S_1(vdW) \rightarrow$ CT. Saigusa and Lim,[6] also using 1-cyanonaphthalene (1-CNN), showed that the shift in the excitation spectrum upon vdW formation depended on the size of the amine complexed, not its ionization potential. This observation indicates that the stability of the complex is determined by the dispersion interaction. In 1-CNN−amine complexes, the larger amines have a smaller spectral shift relative to the band origin, for example, 29 cm^{-1} for trimethylamine down to −6 cm^{-1} for tripropylamine. A similar but greater trend is true for naphthalene−amine complexes. We observed (see below) a 19-cm^{-1} shift in trimethylamine and −28 to −30-cm^{-1} shift in triethylamine (see also Bisht et al.[7]). By contrast, the observation of exciplex fluorescence depends on the ionization potential of the amine, and as might be expected for an electron-transfer reaction, a high ionization potential relative to the acceptor is found to be energetically unfavorable.[8] The exciplex emission has a characteristically broad quasi-Gaussian shape in each of the complexes studied, and the shape and wavelength of maximum emission are largely independent of excitation wavelength in any one type of complex.

The CT complexes have been classified into three cases with the parameter $\Delta = I_D + E_A - E_{S1}$, where I_D is the ionization potential of the donor, E_A is the electron affinity of the acceptor, and E_{S1} is the excited-state energy of the acceptor. Large values of Δ, >4.5 eV, correspond to the case in which the LE state is lowest in energy for excitation from the ground-state vdW complex and there is weak interaction between donor and acceptor. The second case occurs when Δ < 3.5 eV and the CT state is lowest in energy. In the third, intermediate, case both species are similar in energy and, consequently, interact strongly.[9]

We report here on the formation, decay, and geometry of the CT complex between naphthalene and trimethylamine (N−TMA) and compare it to the triethylamine complex (N−TEA).

Experimental Details

A supersonic expansion was made by expanding a mixture of naphthalene and amine, diluted in helium, through a nozzle with a pinhole of 100 μm. The nozzle contained a heated, stainless-steel-crucible reservoir (118 °C) for the naphthalene, through which the helium backing gas (helium, 99.95% BOC) was made to flow. The nozzle tip was independently heated to

* To whom correspondence should be addressed. E-mail: Godfrey.Beddard@chem.leeds.ac.uk.

‡ Premanent address: Unilever Research, Quarry Road East, Bebington, Wirral CH63 3JW, U.K.

10.1021/jp0010334 CCC: $19.00
Published on Web 07/29/2000

ca. 10 °C more than the reservoir in order to prevent clogging and was positioned so that the expanded jet of molecules moved perpendicularly to the direction of the excitation laser. Fluorescence was collected by a fused-silica condenser ($f = 25$ mm, Melles-Griot 01-CMP 111) arranged perpendicularly to both the laser and the molecular beam axes and focused 2−3 mm below the nozzle so that $x/d = 20-30$. Care was taken to minimize the laser scatter in the chamber by baffling the laser light as it entered and exited the apparatus. A high-throughput 250 m^3 hr^{-1} pump (Edwards EH250-ED660) was necessary to keep the background pressure at approximately 10^{-1} mbar.

The liquid amines were introduced into the gas flow by bubbling the helium through an ice-cooled reservoir external to the vacuum chamber. Triethylamine (TEA) (99%, Lancaster) was used as the pure liquid and trimethylamine (TMA) as an aqueous solution (25−27 wt %, Aldrich) in a manner similar to that of Saigusa and Lim.[8] Because of the high vapor pressure of the pure liquid TMA, an aqueous solution was used, which made the concentration of the TMA in the jet easier to control. The relative concentration of the amine was adjusted by varying the bubble rate through the reservoir with a precision-needle valve (Hoke) until the fluorescence signal from the complex was maximized. We had previously attempted to observe naphthalene−water clusters but were unable to detect a signal. The jet of naphthalene was characterized spectroscopically to ensure that the expansion conditions were adequate. Vibrational hot bands were not significant unless the backing pressure was much lower than that normally used, 4.5 bar. It was shown that at lower amine concentrations the fluorescence-excitation spectrum was unaltered, demonstrating the absence of larger clusters in the jet. Adding an excess of amine reduced the relative intensity of the N−TMA complex signal and added extra peaks to the FE spectra, presumably due to N−$(TMA)_n$ clusters.

Two types of lasers and detection methods were employed. To investigate the fast response of the fluorescence, a home-built, time-correlated, single-photon counting instrument (TC-SPC) was used. The fwhm of the instrumental response was 56 ps with a microchannel plate photomultiplier (Hamamatsu R1564U-01). The source was a cavity-dumped dye laser operating with Rhodamine 6G and which produced pulses of ∼2-ps duration when pumped by a frequency-doubled, mode-locked Nd:YAG laser (Spectron SL03ML). Prior to entering the vacuum chamber, the laser pulses were frequency-doubled by an angle-tuned $LiIO_3$ crystal and filtered to remove fundamental light. The wavelength of the frequency-doubled light was calibrated with a SPEX 1702/04 monochromator and the spectral width was measured to be 5 cm^{-1}. In principle, there is an uncertainty associated with measuring the decay of long-lived species due to movement of excited molecules out of the focal region of the collecting lens. This effect was small, because the literature value[10] for the naphthalene fluorescence decay lifetime of 318 ns was obtained for the $8(b_{1g})^1$ transition.

The laser source used for fluorescence excitation and dispersed fluorescence experiments was a Spectron dye laser (SL4000G) pumped by a Q-switched Nd:YAG laser (Spectron 6L803) using Kiton Red as the dye. This produced 10-ns pulses between 308 and 321 nm after frequency doubling and with a bandwidth of 0.15 cm^{-1}. The light from the Q-switched dye laser was not focused into the source chamber, and experiments were performed to verify that the absorption of the naphthalene was not being saturated. The emission collected was filtered with a 308-nm 0° HR mirror (TecOptics) and a WG330 Schott glass filter, then it was focused by a lens onto the slits of a 2-m monochromator (Spex 1702/04). A fast photomultiplier (Philips XP2020Q) was placed at the exit slits, and the entire anode signal from the photomultiplier was sampled by a boxcar integrator (Stanford Research SR250). Typically, 30−100 signals were averaged. A photodiode detector (RS 194-076, OSD15-5T) with a matching boxcar integrator corrected for the laser intensity fluctuations. Longer, nanosecond, decays could also be recorded by using an oscilloscope (Tektronix TDS 460) instead of a boxcar. The time resolution was 2 ns, and typically, 256 profiles were averaged for each decay lifetime. At times longer than about 400 ns, the effects of fly-out could be observed. When measuring the fluorescence-excitation spectra, the signal was sampled near the peak of the fluorescence spectrum through the monochromator with a bandwidth, set by the slit width, of ∼3 nm; centered at 318 nm for naphthalene, 375 nm for N−TMA, and 395 nm for N−TEA.

The ground-state geometry of the vdW complex was estimated using standard quantum chemistry methods, initially by density functional theory, B3YLP/aug-cc-pVDZ, and then by MP2/cc-pVDZ. These results, which are described in more detail below, were helpful in the interpretation of the band profiles observed in the fluorescence-excitation spectra.

Results

Excitation Spectra. The fluorescence-excitation spectrum (FES) of jet-cooled naphthalene and the N−TMA complex excited on the $S_1(^1B_{3u}) \leftarrow S_0(^1A_g)$ electronic transition is shown in Figure 1. The wavenumber scale is relative to the weak naphthalene O−O band origin (not shown) at an excitation energy of $h\nu \times 32020$ cm^{-1} (312.30 nm), and the intensity of each spectrum was normalized with respect to the first b_{1g} symmetry vibrational band at either ∼435 (naphthalene) or ∼455 cm^{-1} (N−TMA), respectively. In naphthalene, the relative intensities of the peaks do not match exactly those reported previously by Behlen et al.[11] due to the difference in detection methods. In our case, we filtered the fluorescence with a monochromator with ∼3-nm-wide slits centered on 318 nm (31 447 cm^{-1}); otherwise, the spectra agree well.

The N−TMA excitation spectrum was recorded at 385 nm. However, the naphthalene spectrum was not completely removed by the filters, so the stronger naphthalene peaks are also weakly seen, but at reduced intensity, and are readily accounted for because of their known wavelengths. The spectrum of the complex is generally blue-shifted by 19 cm^{-1} relative to the corresponding band of the naphthalene spectrum, which is in the opposite sense to that observed in the related N−TEA complex, where a 28−30-cm^{-1} red shift is observed.[7] The N−TMA excitation spectrum appears to exhibit a short progression built on the intramolecular vibration. This appears as a low-frequency mode, at +30 cm^{-1} from the 455-cm^{-1} line and at +25 from the 726-, 931-, and 1162-cm^{-1} lines, but not from the 525-cm^{-1} line. Additionally, weaker bands at +50 cm^{-1} from the 455-, 526-, and 1161-cm^{-1} lines are present but are either absent or too weak to be seen from the 726- and 931-cm^{-1} lines. Tentatively assuming that these series of lines are the first two of a progression in a Morse potential, then $\omega_e = 28 \pm 2$ cm^{-1} and $x_e = 0.13 \pm 0.02$ and the intermolecular dissociation energy of the initially excited vdW complex is ∼60 cm^{-1}, which would explain why more lines are not observed, but does not agree with our ab initio calculations, which suggest that the vdW well depth is at least an order of magnitude greater.

Rotational Structure. Figure 2 shows the naphthalene $8(b_{1g})^1$ band and the corresponding band in N−TMA in more detail. From the measured rotational constants,[12] we were able to

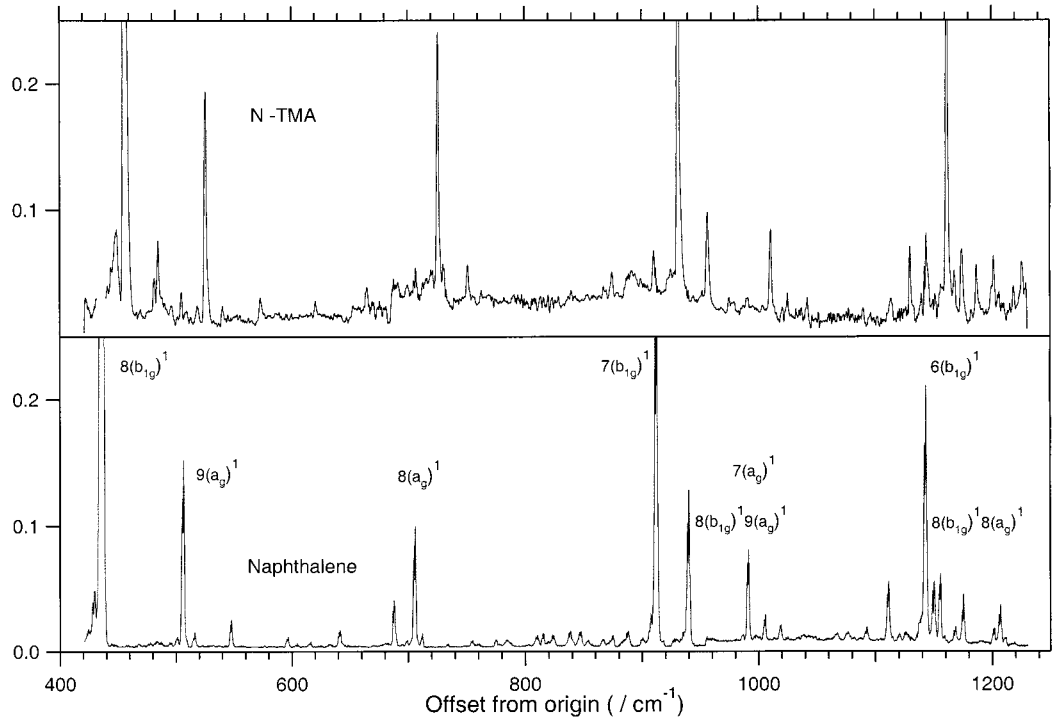

Figure 1. $S_1 \leftarrow S_0$ fluorescence excitation spectra of naphthalene and the N−TMA vdW complex. The excitation energy is shown relative to the naphthalene O−O band origin (32020 cm^{-1}). The spectral intensity is normalized to the vibronic transitions at about 435 (N) or 455 cm^{-1}(N−TMA). The N−TMA origin is at 32 040 cm^{-1}.

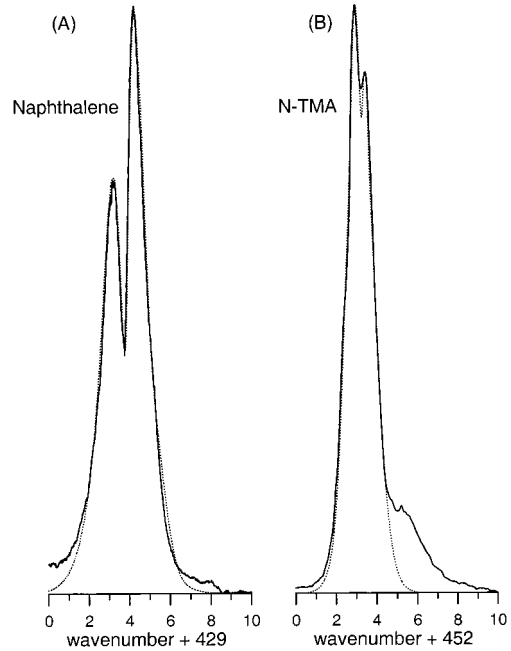

Figure 2. (A) Rotational contours of the naphthalene 435 cm^{-1}, $8(b_{1g})^1$, transition and (B) 455-cm^{-1} transition in N−TMA. The solid line is the data and the dotted line is the fit.

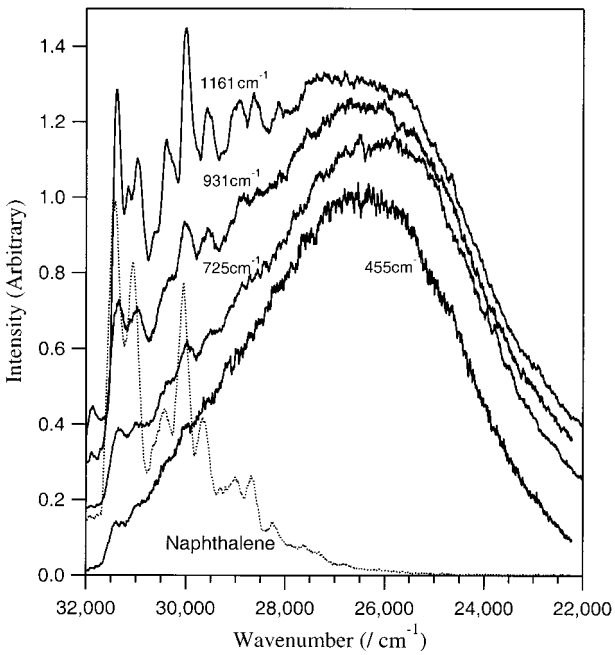

Figure 3. Dispersed fluorescence spectra from N−TMA. Spectra were recorded respectively at 455, 725, 931, and 1161 cm^{-1} above the naphthalene band origin. These correspond to the four strong cluster absorptions seen in Figure 1.

synthesize and fit the naphthalene rotational contour, the only free parameter being the temperature. In this way, we calculated that the molecular beam had an effective rotational temperature of 6 ± 2 K. The rotational structure observed in N−TMA is in contrast to N−TEA, where none is visible at the resolution of our laser, even though the fwhm of the vibrational features are similar in each case: 2.2 cm^{-1} in naphthalene, 1.8 cm^{-1} in N−TEA, and 1.5 cm^{-1} in N−TMA.

Fluorescence Spectra. Figure 3 shows dispersed fluorescence spectra of the N−TMA dimer, recorded at four different excitation energies, 455, 725, 931, and 1161 cm^{-1}, which correspond to excitation into the major cluster absorption features shown in Figure 1. Emission from the origin was too weak to be measured reliably. In marked contrast to the spectrum reported by Bisht et al. for N−TEA clusters[7] and our own measurements, the dispersed N−TMA spectrum shows almost no fluorescence from a locally excited naphthalene-like state when excited at 455 cm^{-1}. The fwhm of the 455 cm^{-1} excited fluorescence is 5300 cm^{-1}, or ∼75 nm wide. The broad red-shifted fluorescence observed in the cluster spectra is highly characteristic of fluorescence from a CT state.

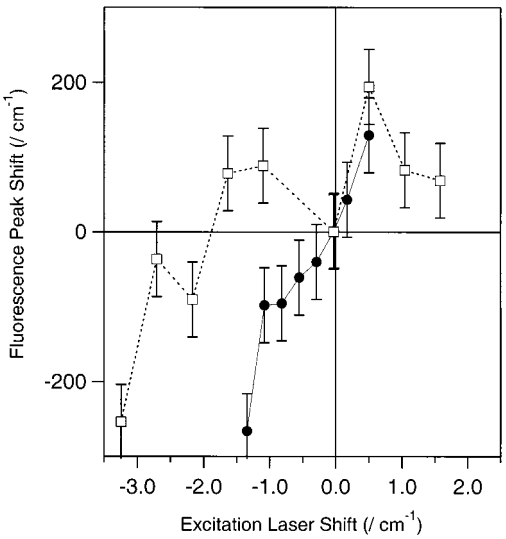

Figure 4. Shift in the wavelength of peak intensity of the CT fluorescence as a function of the laser excitation energy across the vibronic feature at 455 (solid circles) and 725 cm^{-1} (open squares). The shifts are relative to the peak of the rotational contour.

The fluorescence spectra of the complex shown in Figure 3 are normalized to the peak of the CT emission and show that the contribution from naphthalene increases with increasing excitation energy but is always the minor component of the spectrum. The CT components of the spectra are similar in that the wavelength of maximum intensity and the width hardly vary with excitation wavelength. The relative yield of CT emission normalized with excitation spectral line intensity varies slightly, with excitation being, relatively, 1, 1.1, 1, and 0.8 for the 455-, 726-, 931-, and 1161-cm^{-1} lines, respectively. By comparison, the relative fluorescence yield of the CT state to that of naphthalene decreases dramatically and in the opposite sense to that observed in N−TEA or 1-CNN−TEA.

On further investigation, we found that as the excitation frequency was scanned over the rotational contours associated with the $8(b_{1g})^1$ and $8(a_{1g})^1$ vibrational transitions, a marked shift was observed in the CT spectrum, and fitting these spectra to a Gaussian function allows an estimate of the peak wavelength to be made. The peak shift vs excitation frequency is illustrated in Figure 4 , measured relative to the peak of the rotational contour. It is remarkable that such small changes in excitation energy, approximately 0.25 cm^{-1} each, resulted in shifts in the peaks of the CT emission of several hundred wavenumbers.

Excited State Decays. Using the TCSPC apparatus or the nanosecond dye laser and oscilloscope as appropriate, we measured excited-state decays. By exciting the $8(b_{1g})^1$ transition, we obtained decay times of 316 ± 5 ns for bare naphthalene and 28 ± 0.5 ns for N−TEA, which compared well with the 30 ns measured by Bisht et al.[7] The corresponding N−TMA decay has a single decay lifetime of 56 ± 3 ns, which is lengthened to 105 ± 5 ns at 1161 cm^{-1} excess energy. The rate of fluorescence decay decreased linearly with increasing excitation energy above the band origin. The results are summarized in Table 1.

Finally, we measured the rise time of the fluorescence when excited at 455 cm^{-1}. Figure 5 shows the fluorescence rise, together with fitted exponential rises convoluted with the instrument step-function response for an instantaneous rise, one of 60 and one of 100 ps. While there is a large error associated with the fitting, the fwhm of our TCSPC apparatus being 56 ps and comparable to the lifetime of the fluorescence grow-in, we can, nevertheless, estimate the time constant for the appearance of the CT fluorescence as 60 ± 20 ps.

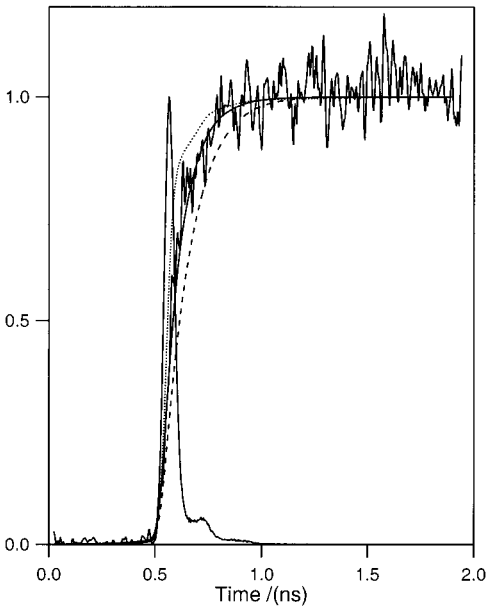

Figure 5. Rise time of the CT-fluorescence signal for the 435 cm^{-1} excitation and instrumental profile. The solid smooth line through the data represents the convolution of the instrument function and a 60-ps rise time. The dotted and dashed lines correspond to rise times of 0 and 100 ps, respectively.

TABLE 1: Decay Lifetimes and Rates of the Exciplex Emission

excitation energy/ hc × cm^{-1}	τ/ns	$k_f/10^6$ s^{-1}
455	56 ± 3	17.9
526	59 ± 3	16.9
725	67 ± 3	14.9
931	92 ± 4	10.9
1161	105 ± 5	9.52

TABLE 2: Rotational Constants Fitted to the N−TMA 455 cm^{-1}

	A″	B″	C″	A′	B′	C′
rotational constant/MHz	901.1	492.1	498.8	914.8	460.9	462.9

Discussion

The excited state behavior of N−TMA has broad similarities to but detailed differences from those of N−TEA and 1-CNN−TEA complexes. Generally, in each type of complex, the excitation spectrum when monitored at the exciplex emission wavelengths consists mainly of the narrow lines of the slightly shifted spectrum of the aromatic molecule upon which weak and short progressions, possibly of an intermolecular mode, are built. Additionally, very weak, underlying broad features centered about the main transitions indicate that some IVR is occurring (see Figure 1). The emission spectrum consists of some aromatic fluorescence at short wavelengths and a broad, featureless exciplex emission at longer wavelengths. The differences in N−TMA compared to other complexes are that the exciplex emission is far greater in proportion to that of the aromatic moiety and that the relative proportion of relaxed fluorescence in the spectrum increases with increasing excitation energy. Also, the exciplex lifetime lengthens with excitation energy, whereas with the N−TEA and 1-CNN−TEA complexes, it shortens.

We attempt to explain our observations as follows: optical excitation promotes the cluster from the electronic ground state to a locally excited (LE) state that has essentially the ground-state geometry and mainly naphthalene character. The LE state can have four competing fates: it may decay by fluorescence from the initially excited vibrational level; it may vibrationally predissociate into excited naphthalene and ground-state TMA and the excited naphthalene may then undergo IVR and, ultimately, fluoresce or suffer intersystem crossing; it may lead directly to the CT state, which is accompanied by geometric isomerization; it may undergo inter- and/or intramolecular vibrational relaxation (IVR), either to levels from which the CT state is formed or to levels producing relaxed naphthalene fluorescence. We now examine these possible outcomes with respect to our observations.

Because the initial, LE, state has largely naphthalene character, it should give rise to some highly structured fluorescence. However, because the formation of the CT state is 60 ps, at 455 cm^{-1} excess energy, and the naphthalene lifetime is 318 ns, the emission yield from the LE state must be very small. This is what is observed in the emission spectrum at low vibrational excitation (see Figure 3), except that more naphthalene emission is observed than predicted: the ratio of CT fluorescence yield to relaxed fluorescence, ϕ(CT)/ϕ(N), is observed to be at least 20 and not more than 100, but is predicted to be 318/0.06 or 5300. This discrepancy, coupled with the observation that the fluorescence lifetime measured in the structured region of the emission is identical to that measured at the peak of the CT component within experimental uncertainty, leads us to conclude that the possibility of the naphthalene-like component's being the result of dissociation into TMA plus excited naphthalene is small. However, this is difficult to prove, because at low excitation energy, there is almost complete CT emission (see Figure 3), and at higher energy, where there is more naphthalene fluorescence, its lifetime is similar to that of the CT state. We cannot say, therefore, whether the complex dissociates, then the naphthalene undergoes IVR, or whether only IVR occurs. Our argument below could be applied to both eventualities.

The small and increasing amount of relaxed naphthalene emission which is observed as the excitation energy increases is attributed to IVR, because each intramolecular vibrational state of naphthalene will be mixed with a large number of low-frequency intermolecular (vdW) vibrational states, and these provide a sufficient density of states to introduce IVR, which results in relaxed fluorescence. The density of the mixed vdW vibrational states increases rapidly with excess vibrational energy of the complex, so one might expect the ratio ϕ(CT)/ϕ(N) to decrease with increasing excitation energy as more relaxed fluorescence is produced. However, mixing of the LE state with the vdW intermolecular vibrations need not only produce excited naphthalene, because we also know[5] that these intermolecular vibrations are the promoting modes for the CT state. The relative amount of CT to relaxed-naphthalene emission at a given amount of excess vibrational energy is explained by competition between the various IVR pathways leading to the CT or naphthalene states. In the cases of 1-CNN−TEA[4] and N−TEA,[7] it seems that IVR leading to the CT state is preferred, because the ratio ϕ(CT)/ϕ(N) is found to increase with excitation energy, whereas our observations in N−TMA suggest that IVR favors formation of excited naphthalene.

Figure 6 shows a plot of ϕ(CT)/ϕ(N) vs excess vibrational energy. This ratio decreases in N−TMA and increases in 1-CNN−TEA and also N−TEA. This differing behavior can

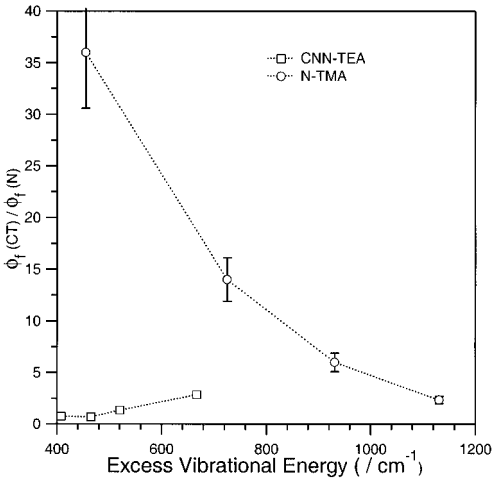

Figure 6. Plot of the quantum yield ratios of CT-to-naphthalene emission as a function of excess vibrational energy.

be rationalized by considering the ratio of the IVR rate constants leading to the CT state and to relaxed fluorescence. For example, at low excess vibrational energy, IVR is relatively slow and the amount of CT emission is determined by the coupling to that state and is greater in N−TMA than in N−TEA. As the excess vibrational energy increases, not only do we move away from the crossing poin, but IVR also increases. If the IVR pathways are more favorable to the CT state, then the ratio of CT-to-relaxed fluorescence will increase, as in N−TEA and 1-CNN−TEA. But if the couplings are disfavored, the opposite occurs, and more relaxed fluorescence will be observed, as in N−TMA.

The rapid rise time of the CT emission in N−TMA is mirrored in N−TEA for the 432- and 702-cm^{-1} transitions, where its measurement[7] was instrumentally limited at <1 ns. However, at the origin the rise time is far longer, 17 ns, and also at 908 cm^{-1}, where it is 12 ns, and decreases to 3 ns at 1419 cm^{-1}. In 1-CNN−TEA[5], exciting the 454-cm^{-1} transition leads to a far-slower 5-ns rise time, but unfortunately, values at other excitations have not been reported. We explain the slow CT fluorescence rise time at low excess energy as being due to tunneling, because the barrier cannot be reached. At and above the threshold, the rise times are explained by Landau−Zener curve crossing. A sufficient amount of energy to surmount the barrier appears to be about 400 cm^{-1} in N−TMA and N−TEA. At threshold, the crossing will be adiabatic and its probability close to unity; hence, the CT rise time will be fast, that is, picoseconds. With more energy, the crossing becomes non-adiabatic, because the kinetic energy along the reaction coordinate increases, and the rate constant decreases. In N−TEA, the decrease in rise time, from 12 to 3 ns as more excess vibrational energy is added, can be explained by the increase in the density of states. Even though we were unable to observe the rise time directly for any state other than the 455-cm^{-1} line, rotational structure is observed in on all major lines in the N−TMA fluorescence excitation spectrum, indicating that no very fast, ≤ ca. 4 ps, crossing occurs as the excess energy increases.

The relatively larger amount of CT emission vs relaxed naphthalene fluorescence in N−TMA vs N−TEA at low excess vibrational energy is, we propose, explained by a larger coupling between the CT and the LE states in N−TMA than in N−TEA. This may be due to the smaller size of the TMA, allowing stronger interaction with the naphthalene ring. Consequently, the crossing point to the CT state in N−TMA should be lower down on the surface and at shorter range than in N−TEA.

While we do not know the reaction coordinate leading to the CT state, we can reasonably argue that it should coincide with the intermolecular separation between the naphthalene and the TMA, as measured from their respective centers of mass. In this way, if we treat the ionic species in the CT state as structureless particles, we can approximately estimate the intermolecular distance at which the CT state crosses the LE state by using the relative ionization potential (IP) of the donor (TMA) and the electron affinity (E_A) of the acceptor. Tobita et al.[13] measured the E_A of naphthalene in low-energy electron-capture experiments and conclude that it is <-0.06 eV. The IP of TMA is 7.82 eV.[6] Denoting the energy of the S_1 locally excited state in the dimer as E_1, and assuming that the ionic potential is essentially Coulombic, and that the intramolecular potential is flat, we can estimate the crossing point, R, as

$$\frac{-14.35}{R} = E_A - \mathrm{IP} + E_1 \qquad (1)$$

where energies are in eV and R is in Å. We know from our measurements that E_1 is 4.02 eV, measured from the energy minimum in the ground state, from which we estimate $R \sim 3.8$ Å. As expected, this is considerably shorter than the intermolecular distance either in the ground state or of the LE state of the complex, which we estimate from ab initio calculations or from our fit to the rotational contours of the FES (see below).

In solution, the fluorescence resulting from the CT state is red-shifted, due to the fact that this state is more strongly bound than the locally excited state. However in the gas phase, the CT state possesses considerable vibrational energy on formation. Furthermore, the CT state is formed near its outer turning point because the LE state exhibits a longer intermolecular bond than the CT state. Once formed, the CT state will have a high density of states into which energy can flow, making the back-transfer to the LE state unlikely during the excited-state lifetime. The wavelength dependence of the CT fluorescence is produced by the projection of the upper-state wave function onto the lower state in the Franck−Condon region (at the inner turning point). The emission is approximately Gaussian in shape, very broad, fwhm 5600 cm^{-1}, and has the same shape and spectral maximum virtually independent of excitation energy. Because the spectra are almost identical for each excitation energy (see Figure 3), it is tempting to suggest that the emission always arises out of the same CT vibrational level, but this is impossible, because the emission lifetime changes with excitation energy: 56−110 ns (see Table 1). Furthermore, the spectra are recorded in a collision-free environment, and it is impossible for the initially excited CT level to decay into a common level, because there is no energy sink.

We attribute the change in the lifetime to a change in the radiative rate of the CT emission with excitation energy. The radiative rate is proportional to the transition dipole and transition frequency as $\nu^3|\int\psi_{CT}\psi_g|^2$. The frequency change is comparably small (at most, 700 in 32 000 cm^{-1}), but the transition dipole to the repulsive ground state becomes smaller as the vibrational quantum number in the CT state increases. This is easily understood if we model the CT state as an anharmonic well (in the intermolecular stretching coordinate) due to the changing size of the wave function's lobes at the (inner) turning point and its consequent overlap with the continuum wave function in the ground-state potential. The lack of wavelength dependence is explained if the repulsive wall in the CT state and the dissociative ground state are approximately parallel.

Rotational Structure. Rotational structure was observed for all of the vibrational transitions in N−TMA. The shape of the band profile is of two types, depending on the symmetry of the excited vibronic mode, and correlates with those found in naphthalene, i.e. *a*-type and *b*-type. This is in contrast to the vibrational transitions of N−TEA, which exhibit no structure at our, and Bisht et al.'s,[7] resolution. In Figure 2 we show the rotational contour for the N−TMA cluster at 455-cm^{-1} excitation, together with a simulation of the rotational spectrum (solid line). We interpret this spectral feature as due to the excitation of an LE state of a naphthalene-like vibration of the complex, corresponding to the $8(b_{1g})^1$ mode in the isolated molecule, superimposed over an underlying, weaker, and broader feature. This broad feature is emphasized by the fit to the data. The origin of the underlying transition is uncertain, but it is unlikely to be due to a cluster of the form N−$(TMA)_2$, because we would expect a spectral shift slightly less than twice that of N−TMA. One possibility is that it is the signature of N−TMA clustered with He, although this feature was not seen to alter with a change in the pressure of helium. Another interpretation, which we favor, is that it is due to another geometric isomer of N−TMA. Supporting this hypothesis is the very large shift we observe in the peak of the CT fluorescence as the frequency-excitation laser is scanned over the spectral feature (see Figure 4).

Assuming that the main feature, Figure 2B, is due to a single conformer of the LE state, we have fitted this to extract the rotational constants of the ground and excited states, having first removed the broad underlying feature by fitting this to a separate Gaussian function and subtracting the result. In fitting these data, we fixed the temperature of the cluster at 6 K, according to the measured rotational temperature of naphthalene in the beam, and then allowed the six rotational constants to vary freely, assuming a *c*-type transition. The rotational profile was simulated by first calculating a stick spectrum using the ASYROT package[14] and then convoluting this with a Lorenztian (0.15 cm^{-1} fwhm). The simulated profile was then compared to the experimental profile, and the rotational constants were varied using a least-squares gradient-optimization routine to minimize the difference. Because the resulting *B*- and *C*-axis rotational constants are almost identical, we cannot say for certain whether the transition is of *b*- or *c*-type. The two transitions in naphthalene are of *a*- and *b*-type, but the presence on the amine changes the axes so that the naphthalene transition dipole lies along the *B* and *C* axes.

This particular combination of measured rotational constants instantly limits the conformational space that the cluster must fit into. One restriction is that the TMA may not lie directly over the center-of-mass of the naphthalene plane. Nor may it lie along the short axis of the naphthalene. By varying the relative geometry of the naphthalene to the amine, we have attempted to refine the geometry by matching the fitted rotational constants to a model structure. The initial geometry was taken from the ab initio calculations described below. We then allowed the molecular components of the cluster to move relative to one another. The region of minimum error between the experimental and the modeled rotational constants is shown in Figure 7 as a contour plot looking down on the naphthalene rings. The relative geometry is such that the amine is slightly over one of the naphthalene rings and is tilted so that only two of the methyl groups' hydrogen atoms point toward the ring (see below). The contours cover the region 2.5 times the minimum χ^2 error, and the rotational constants obtained were 464, 518, and 932 MHz, compared to experimental values of

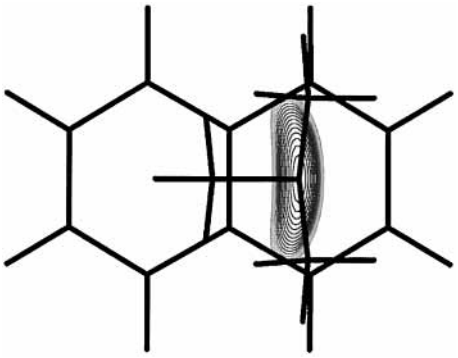

Figure 7. Contour fit and geometry of the N−TMA complex. The contour levels measure the relative error in fit to the rotational constants as the amine is translated across the plane of the naphthalene rings in 0.05 Å steps. The intermolecular separation between the amine and the naphthalene moieties was optimized by similar calculations. The outside contour is 2.5 times the minimum error.

492, 499, and 901 MHz. The nitrogen atom is 4.08 Å from the plane of the naphthalene.

We are uncertain why we observed rotational structure in N−TMA but not in N−TEA. Obviously, the rotational constants in N−TEA are smaller than those in N−TMA, so the rotational contour might simply not be resolvable with our laser (line width, ∼0.15 cm^{-1}), but it is also possible that the lifetime of the N−TMA is longer than that of N−TEA, which might be lifetime-broadened. The rotational features in both complexes have a similar width, ∼1.8 and ∼1.5 cm^{-1} for N−TMA and N−TEA, respectively, which, if the latter were lifetime-broadened by rapid transfer to the CT state or by IVR, would have a lifetime of ∼3.5 ps. By comparison to other data, this lifetime would seem to be too short. Bisht et al.[7] measured the CT signal rise times in N−TEA, and these are generally much slower (∼3−17 ns), although unfortunately, they were unable to measure the rise times of the $8(b_{1g})^1$ and $9(a_g)^1$ modes to better than <1 ns. We conclude that the lack of obvious structure in the N−TEA profiles is probably not due to homogeneous broadening.

To confirm the geometry of the vdW dimer, we performed structural calculations on the ground-state species using ab initio methods.[15] The geometry was initially estimated by a density functional method, B3YLP/aug-cc-pVDZ. This was used as the input geometry to an MP2/6-31G calculation and subsequently refined by extending to MP2/cc-pVDZ to obtain the final geometry. As is to be expected, the inclusion of electron-correlation and diffuse functions led to a stabilization of the cluster, because the dispersion interaction was increasingly better-modeled. The geometries of the molecular moieties changed only slightly with the sophistication of the level of theory. The cluster geometries predicted by the density functional theory and the Møller−Plesset perturbation theory were similar, except that the amine became more tilted with respect to the ring in the MP2 calculations. By adding more diffuse functions, the intermolecular distance was substantially reduced. The final MP2/cc-pVDZ geometry is shown in Figure 8. The major difference between this geometry and that arrived at by fitting the experimental rotational constants is that the intermolecular separation of the later, at 4.08 Å, is shorter by 0.25 Å. This is quite reasonable, given the relatively small basis set used in the calculations. Note that this is much longer than the intermolecular separation expected at the crossing point between the LE and CT surfaces, which we estimate (above) to be 3.8 Å. We checked whether the later geometry might not have been another local minimum by starting the ab initio optimization

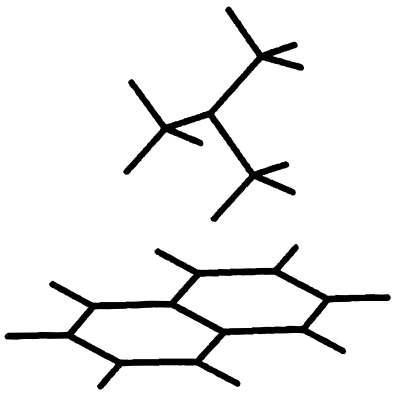

Figure 8. View of the optimized geometry, calculated at the MP2/cc-pVDZ level of theory.

calculation with these coordinates, but found that the complex moved back to the previously calculated position. When we took account of basis set superposition error[16] using the standard counterpoise correction,[17] we found the vdW stabilization energy, neglecting any zero-point energy correction, to be 726 cm^{-1}. In reality, it is probably greater than this because of basis set limitations.

We do not have an easy explanation for the remarkable shift that we observed in the peak of the CT emission spectrum as we scanned over the 455- or 725-cm^{-1} vibrational modes. It is clear from Figure 2B that the 455-cm^{-1} mode overlaps another relatively broad spectral feature, which is probably due to another conformer or larger cluster. It is likely that as we scanned across the rotational contour we excited an increasingly larger amount of this other conformer, which might account for the shift in the fluorescence maximum. The dispersed spectra also showed an increasingly larger proportion of naphthalene-like emission as the excitation energy was scanned into the blue wing of the 455-cm^{-1} rotational contour. It is, therefore, possible that the unidentified species dissociates into excited-state naphthalene more easily than it undergoes charge transfer, and the lack of rotational structure in the underlying spectral feature might be considered as supporting evidence for this.

Conclusions

The photophysics of the jet-cooled N−TMA vdW complex has been studied using fluorescence excitation and emission spectroscopy. The N−TMA complex has absorption transitions of a naphthalene-like nature that are blue-shifted by ∼20 cm^{-1} from pure naphthalene. Rotational profiles are observed on the main transitions and fitted with constants of 499, 492, and 901 MHz. These constants are consistent with a geometry of the complex with the amine disposed symmetrically above one of the naphthalene rings, with the hydrogen atoms pointing toward the ring, and with an intermolecular separation of 4.00 Å (see Figure 7). The structure was obtained by fitting the geometry to the rotational constants and also by ab initio calculations which are in good agreement (see Figure 8). The related N−TEA complex has in contrast red-shifted transitions compared to naphthalene, and although measured to similar resolution, no rotational profiles could be resolved.

The emission spectrum shows both naphthalene and CT features but in varying proportions, depending upon the excitation energy. The two types of emission are attributed to naphthalene-like relaxed emission from a state with almost pure naphthalene character and a CT-state emission with almost no naphthalene but a large amount of ionic character. The two states are coupled by IVR. How this distributes energy about the

complex is used to explain the differing ratios of CT-to-relaxed fluorescence with excess vibrational energy in N−TMA as compared to N−TEA and CNN−TEA.

Acknowledgment. We acknowledge the support of the Royal Society and the EPSRC. D.P.A. acknowledges the support of an EPSRC postgraduate studentship award. We are grateful to Dr. H. Qian for assistance with the fitting of the rotational constants to the band contours.

References and Notes

(1) Russell, T. D.; Levy, D. H. *J. Phys. Chem.* **1982**, *86*, 2718−2727.
(2) Castella, M.; Prochorow, J.; Tramer, A. *J. Chem. Phys.* **1984**, *81*, 2511−2512.
(3) Saigusa, H.; Itoh, M. *Chem. Phys. Lett.* **1984**, *106*, 391−394.
(4) Saigusa, H.; Itoh, M. *J. Chem. Phys.* **1984**, *81*, 5692−5699.
(5) Saigusa, H.; Itoh, M.; Baba, M.; Hanazaki, I. *J. Chem. Phys.* **1987**, *86*, 2588−2596.
(6) Saigusa, H.; Lim, E. C. *J. Phys. Chem.* **1991**, *95*, 7580−7584.
(7) Bisht, P. B.; Petek, H.; Yoshihara, K. *Chem. Phys. Lett.* **1993**, *213*, 75−83.
(8) Saigusa, H.; Lim, E. C. *J. Phys. Chem.* **1991**, *95*, 1194−1200.
(9) Castella, M.; Millie, P.; Piuzzi, F.; Caillet, J.; Langlet, J.; Claverie, P.; Tramer, A. *J. Phys. Chem.* **1989**, *93*, 3949−3957.
(10) Behlen, F. M.; Rice, S. A. *J. Chem. Phys.* **1981**, *75*, 5672−5684.
(11) Behlen, F. M.; McDonald, D. B.; Sethuraman, V.; Rice, S. A. *J. Chem. Phys.* **1981**, *75*, 5685−5693.
(12) Majewski, W.; Meerts, W. L. *J. Mol. Spectrosc.* **1984**, *104*, 271−281.
(13) Tobita, S.; Meinke, M.; Illenberger, E.; Christophorou, L. G.; Baumgartel, H.; Leach, S. *Chem. Phys.* **1992**, *161*, 501−508.
(14) Birss, F. W.; Ramsay, D. A. *Comput. Phys. Commun.* **1984**, *38*, 83.
(15) Frisch, M. J.; Trucks, G. W.; Schlegel, H. B.; Scuseria, G. E.; Robb, M. A.; Cheeseman, J. R.; Zakrzewski, V. G.; Montgomery, J. A.; Stratmann, R. E.; Burant, J. C.; Dapprich, S.; Millam, J. M.; Daniels, A. D.; Kudin, K. N.; Strain, M. C.; Farkas, O.; Tomasi, J.; Barone, V.; Cossi, M.; Cammi, R.; Mennucci, B.; Pomelli, C.; Adamo, C.; Clifford, S.; Ochterski, J.; Petersson, G. A.; Ayala, P. Y.; Cui, Q.; Morokuma, K.; Malick, D. K.; Rabuck, A. D.; Raghavachari, K.; Foresman, J. B.; Cioslowski, J.; Ortiz, J. V.; Stefanov, B. B.; Liu, G.; Liashenko, A.; Piskorz, P.; Komaromi, I.; Gomperts, R.; Martin, R. L.; Fox, D. J.; Keith, R.; Al-Laham, M. A.; Peng, C. Y.; Nanayakkara, A.; Gonzalez, C.; Challacombe, M.; Gill, P. M. W.; Johnson, B. G.; Chen, W.; Wong, M. W.; Andres, J. L.; Head-Gordon, M.; Replogle, E. S.; Pople, J. A. *Gaussian 98* (Revision A.7); Gaussian, Inc.: Pittsburgh, PA, 1998.
(16) Jensen, F. *Introduction to Computational Chemistry*; John Wiley: Chichester, 1999.
(17) Boys, S. F.; Bernardi, F. *Mol. Phys.* **1970**, *19*, 553−556.